

Determination of the internal state distribution of NO produced from the H+NO₂ reaction

Deborah G. Sauder and Paul J. Dagdigian

Citation: *The Journal of Chemical Physics* **92**, 2389 (1990); doi: 10.1063/1.457981

View online: <http://dx.doi.org/10.1063/1.457981>

View Table of Contents: <http://scitation.aip.org/content/aip/journal/jcp/92/4?ver=pdfcov>

Published by the [AIP Publishing](#)

Articles you may be interested in

Chemiluminescent reactions of group 2 (Ca, Sr, and Ba) elements with H₂O₂, tBuOOH, HNO₃, and NO₂: Reactivities and product state distributions

J. Chem. Phys. **100**, 2637 (1994); 10.1063/1.466459

Radical addition to HNO. Ab initio reaction path and variational transition state theory calculations for H+HNO→H₂NO and H+HNO→HNOH

J. Chem. Phys. **99**, 7709 (1993); 10.1063/1.465700

A laserinduced fluorescence determination of the internal state distribution of NO produced in the reaction: H+NO₂→OH+NO

J. Chem. Phys. **93**, 3187 (1990); 10.1063/1.458851

A laserinduced fluorescence determination of the complete internal state distribution of OH produced in the reaction: H+NO₂→OH+NO

J. Chem. Phys. **93**, 3177 (1990); 10.1063/1.458850

Laserinduced fluorescence determination of internalstate distribution of OH produced by H+NO₂ in crossed molecular beams

J. Chem. Phys. **65**, 1811 (1976); 10.1063/1.433273



Determination of the internal state distribution of NO produced from the H + NO₂ reaction

Deborah G. Sauder and Paul J. Dagdigan

Department of Chemistry, The Johns Hopkins University, Baltimore, Maryland 21218

(Received 30 January 1989; accepted 17 November 1989)

The internal state distribution of the NO product from the H + NO₂ reaction was determined in a crossed-beam experiment. Rotational populations in the $v = 0$ to 2 vibrational levels of NO were derived from laser fluorescence excitation spectra of the $A^2\Sigma^+ - X^2\Pi$ band system. The vibrational distribution decreases monotonically with v , and the rotational state distribution is peaked at low J (most probable J of approximately 11.5), but the tail of the distribution extends out to $N \approx 50$. After correction for the flux-density transformation, the vibrational population distribution is found to equal $1:0.17 \pm 0.04:0.05 \pm 0.02$ for $v = 0, 1, 2$, respectively. The lower F_1 ($\Omega = 1/2$) spin-orbit component is preferred over the F_2 ($\Omega = 3/2$) manifold by a ratio of $1:0.52 \pm 0.11$, independent of vibrational level. At high J , a preference for the $\Pi(A')$ Λ doublet levels is observed. Approximately $9.5\% \pm 2\%$ of the reaction exoergicity is found in NO internal excitation. The NO and previously determined OH internal state distributions are compared with statistical distributions calculated by phase-space theory. The energy disposal in OH is found to be greater than statistical, while the opposite is true for NO, as might be expected in a direct reaction of the type $A + BCD \rightarrow AB + CD$ for the "new" and "old" bonds, respectively. The Λ doublet preference observed here for the NO product, and previously for the OH product, can be explained by the dissociation of an HONO(\tilde{X}^1A') intermediate. A mechanism for the generation of unequal NO spin-orbit populations, involving nonadiabatic mixing in the exit channel, is proposed.

I. INTRODUCTION

The H + NO₂ \rightarrow OH + NO reaction is fast and exothermic ($\Delta H_0^\circ = -123.50 \pm 1.99$ kJ/mol, using heats of formation from a recent compilation¹) and plays a role in various combustion environments. The thermal rate constant for this reaction has been measured by a number of different groups²⁻⁴ and equals approximately 1.3×10^{-10} cm³ molecule⁻¹ s⁻¹ at 298 K. This process has also been widely used to prepare OH radicals in flow kinetic studies since it quantitatively converts hydrogen atoms to hydroxyl radicals.⁵ Also, it is an example of a reaction involving *two* open-shell reactants. Since NO₂ is a stable free radical, H + NO₂ is relatively easy to study compared to other atom-radical reactions. The approach of a hydrogen atom to NO₂ (\tilde{X}^2A_1) yields two potential-energy surfaces, which in planar geometry can be classified as $^1A'$ and $^3A'$. It is expected that the reaction proceeds along the $^1A'$ surface, possibly accessing the deep minima corresponding to the *trans* and *cis* forms of the ground \tilde{X}^1A' state of nitrous acid, HONO.⁶ It has been argued⁷ that the $^3A'$ surface does not play a role in the reaction and most likely possesses a barrier much larger than the incident translational energy.

There have been a number of previous experimental studies of the dynamics of this reaction, and considerable information is available on the energy disposal into the translational and OH internal degrees of freedom. The translational energy disposal has been found in crossed-beam experiments to be $\sim 25\%$ of the reaction exoergicity by two different groups.^{8,9}

The internal state distribution of the OH product has been studied in a large number of experiments by observa-

tion of the spontaneous infrared emission,¹⁰⁻¹³ laser fluorescence detection,^{7,14-16} and also electron paramagnetic resonance.¹⁷ A summary of the derived OH vibrational state distributions from experiments carried out up to 1987 has been given by Klenerman and Smith.¹³ The distribution is found to fall off monotonically with increasing v , and the average energy in OH vibration is calculated^{12(c)} to be 25% of the reaction exoergicity. The OH rotational distribution has been characterized in laser fluorescence studies,^{7,14-16} and 22% of the reaction exoergicity is found in this degree of freedom. Thus, by difference, we expect 28% of the exoergicity to appear as internal excitation of the NO product.

Both the OH and NO products are open-shell diatomic molecules. The relative populations of the fine-structure levels can lead to further insights in the reaction dynamics. The relative populations of the spin-orbit states of the OH product, i.e., the ratio of the F_1 ($\Omega = 3/2$) to F_2 ($\Omega = 1/2$) populations, is found^{7,16} to be approximately equal for this reaction. However, a preferential production of Λ doublet levels favoring the symmetric $\Pi(A')$ levels over the antisymmetric $\Pi(A'')$ levels^{18,19} by a ratio of 1.5 ± 0.2 to 1, approximately independent of vibration or rotational level, was observed.⁷ The preferential production of the $\Pi(A')$ levels was explained as the result of the role of a planar HONO(\tilde{X}^1A') intermediate.⁷ When the complex falls apart and the central N-O bond breaks, the O($2p\pi$) orbital of the OH product is expected to be doubly occupied in the component perpendicular to the molecular plane, while the in-plane component will be singly occupied. Provided that planarity is maintained throughout the reactive collision, we would expect preferential formation of the $\Pi(A')$ Λ doublet levels of both reaction products.

In contrast to OH, the internal state distribution of the NO product has been much less extensively studied. Infrared chemiluminescence from vibrationally excited NO has been observed, and the NO $v = 1$ to $v = 2$ vibrational population ratio has been found to equal 70:30.¹² Here we present the first report on a determination of the nascent rotational energy distribution in the NO product. These studies were carried out using laser fluorescence excitation detection of NO by means of its $A^2\Sigma^+ - X^2\Pi$ band system in a crossed-beam experiment. Rotational distributions have been determined for $v = 0$ to 2. Relative vibrational populations have been obtained by summing the populations of the rotational states in each vibrational level. As these experiments were nearly completed, we learned of a similar study by Smith and co-workers on a remeasurement²⁰ of the OH internal energy distribution, which focuses on the laser-induced fluorescence detection of OH ($v > 1$) levels, as well as determination of the internal energy distribution in the nitric oxide product.²¹

II. EXPERIMENT

The crossed-beam apparatus in which these experiments were carried out is a modification of the arrangement used to study NH₂ and NH(X, a) rotationally inelastic collisions and has been described in detail previously.²² Molecular beams of the two reagents were prepared in two differentially pumped chambers abutting the reaction chamber at right angles; these beams cross at a 90° intersection angle in the reaction chamber 2.5 cm beyond their respective skimmers.

Ground-state atomic hydrogen was produced in a microwave discharge supersonic source using an extended Evenson–Broida cavity.²³ This simple arrangement allows adjustment of the discharge without the necessity of complicated mechanical feedthroughs to the cavity; moreover, the length of the tubing (3.2 cm) from the discharge to the beam orifice (0.7 mm diam) could be kept short. A continuous flow of H₂ (typical pressure 3 Torr) with a trace of H₂O added was fed through a 0.7 cm i.d. quartz tube which had been treated with hydrofluoric acid to minimize recombination. The hydrogen beam was collimated with a 0.25 cm diam skimmer. The source chamber was pumped by a water-baffled 6 in. diffusion pump (Varian VHS-6).

The NO₂ (1%–2% in Ar) was fed through a stainless-steel tube to a commercial pulsed solenoid valve (General Valve) with a nozzle diameter of 0.05 cm operated at 10 Hz. Typical backing pressure was 1/2 atm. The NO₂ reservoir was held at room temperature. This source chamber was evacuated by an unbaffled Varian VHS-10 diffusion pump. The NO₂ beam was collimated with a 0.2 cm diam conical skimmer and entered the scattering chamber. We were not able to directly determine the N₂O₄ concentration in our beam; however, we calculate that approximately 3% of the NO₂ is present as N₂O₄ under the conditions in the source reservoir. It is possible that NO₂ polymers could be formed in the supersonic expansion. While we have not made any checks for this, we believe, on the basis of previous experiments with beams of NO₂ seeded in argon (2%–10%) un-

der similar backing conditions,^{7,24} that condensation is not occurring to any significant extent.

The reaction chamber was evacuated by a water-baffled 10 in. diffusion pump (Varian HS-10). The average pressure in the scattering chamber with both beams on was $< 1 \times 10^{-5}$ Torr. The NO product was detected by laser fluorescence excitation in its $A-X$ band system. The appropriate ultraviolet probe radiation was generated by frequency doubling the output of a Nd:YAG (where YAG denotes yttrium aluminum garnet) pumped dye laser and mixing with the 1.06 μm residual fundamental in a commercial laser system (Quantel). The laser was fired typically 100 μs after the opening of the NO₂ pulsed valve. The timing between the valve opening and the laser firing was controlled with a digital delay generator (Stanford Research Systems).

The laser beam, attenuated with a polarizer, passed through the collision zone perpendicularly to both molecular beams. The laser pulse energy was measured at the collision zone with a Molelectron J3 joulemeter and was typically 40 μJ in a 0.4 cm diam collimated beam. Extensive studies of the dependence of the laser-induced fluorescence (LIF) spectra on laser pulse energy were not carried out; however, the relative laser intensities of the (0,0) and (1,1) bands were unchanged with a factor of 5 increase in laser intensity. We believe that we are within the linear response range for LIF excitation since our laser energy density is below the levels for which saturation is predicted to occur according to a crude kinetic model.¹⁴ Moreover, a linear response was verified at even higher laser energy densities per unit bandwidth in other studies involving NO.^{25–27}

Fluorescence excited by the probe radiation was collected through a three-lens telescope whose optical axis was coplanar with and bisected the angle between the two molecular beams. For experimental convenience, the telescope had a 90° bend, which was accomplished with a mirror. Light transmitted through the telescope was detected with an EMI 9813QB photomultiplier, amplified with a charge sensitive preamplifier (Amptek), and fed to a boxcar integrator (Stanford Research Systems). A substantial problem with background visible radiation from the microwave discharge (mainly the hydrogen Balmer line at 656.3 nm) was reduced to tolerable levels by replacing the telescope's aluminized mirror (previously described in Ref. 22) with a 2 in. diam dichroic mirror (Acton) which had $> 90\%$ reflectivity at a 45° angle of incidence over the range from 242 to 279 nm and less than 5% reflectance in the visible. A reflectance curve for the dichroic mirror was provided by the manufacturer and was verified and extended to longer wavelengths by measuring its transmission at a 45° incidence angle. The bend in the telescope allowed the photomultiplier to be conveniently mounted at the end of the telescope tube, perpendicular to the bottom of the vacuum chamber. Spectra were taken under the control of a laboratory microcomputer (DEC LSI-11/23) and subsequently transferred to an Apple Macintosh II for analysis.

III. RESULTS

The total energy E_{tot} available to the products is the sum of ΔH_0° and the internal and translational energies of the

reactants. The reagent energy residing as internal excitation is negligible for the hydrogen atom beam, because of its monoatomic nature, and for the NO₂ reagent, because of the supersonic cooling of this beam. The rotational temperature of NO₂ was not determined, but NO₂ laser fluorescence excitation scans showed a very sparse spectrum characteristic of a rotationally cold beam. The relative translational energy was calculated to equal 3.9 kJ/mol by assuming complete conversion of the stagnation enthalpies of the beams to translational motion and allowing for 1% seeding of NO₂ in argon. This implies that E_{tot} equals 127.4 kJ/mol, implying that rotational levels can be populated up to $N = 78$ in NO($v = 0$), or vibrational levels up to $v = 5$.

Laser fluorescence excitation spectra of the NO product were recorded for the (0,0), (1,1), (2,2) and (0,2) bands of its $A^2\Sigma^+ - X^2\Pi$ band system.²⁸ Figure 1(a) displays a typical spectrum for the (0,0) band with both molecular beams on. A residual laser fluorescence signal was detected in the (0,0) band even when the hydrogen atom beam was turned off by extinguishing the microwave discharge. In principle, this background signal could arise from the photolysis of the NO₂ reagent and subsequent $A-X$ excitation of the NO fragment, or from fluorescence excitation of residual NO in the NO₂ reagent. We believe that the former is the

origin of this signal since the NO background is not rotationally cold ($T \approx 150$ K if the distribution is fitted to a Boltzmann form), as is the case for NO₂. Presumably, this background signal, which should be quadratic with probe laser pulse energy, could have been eliminated by further reduction of the probe laser pulse energy; however, we were not able to do this and still have an adequate signal-to-noise ratio in the NO LIF spectra. The photolysis contribution represented about 50% of the integrated LIF intensity in the spectral region shown in Fig. 1(a). As described below, this background signal was taken into account in the determination of the NO internal state distribution.

Figure 2(a) compares the fluorescence intensities of the high- J lines of the (0,0) band with the (1,1) band. Spectra were also taken to the blue of this region through the heads of the (2,2) band, which was at the shortest wavelength accessible with our laser system. Comparison of the intensities of the (0,0), (1,1), and (2,2) bands allowed determination of the relative vibrational populations of the NO $v = 0-2$ levels. For the estimation of the rotational state distribution in $v = 2$, we employed the (0,2) band, an experimental spectrum of which is displayed in Fig. 3(a). It was not necessary to correct the spectra in Figs. 2(a) and 3(a) for a photolysis contribution since no detectable NO fluorescence signal was observed in these wavelength regions.

The bandwidth of our UV probe laser radiation and the

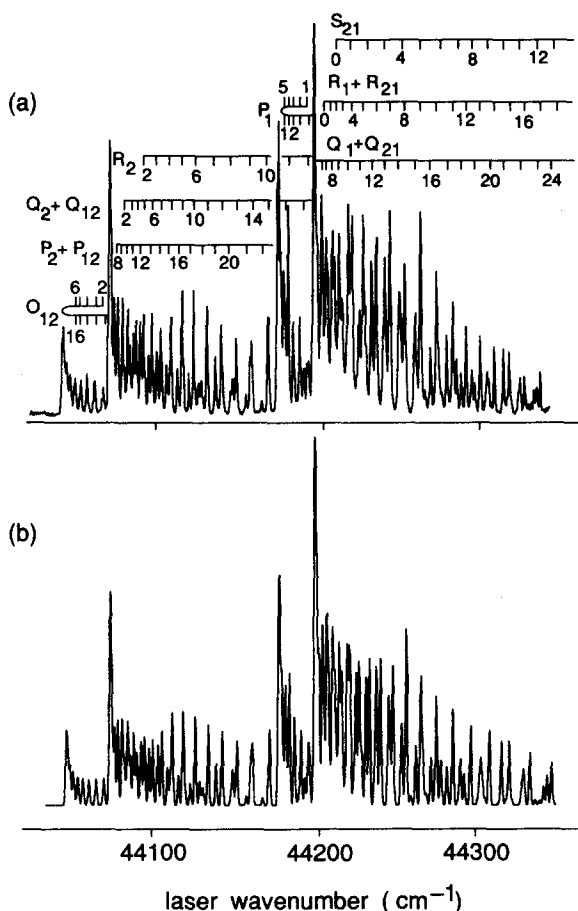


FIG. 1. (a) Experimental laser fluorescence spectrum in the $A^2\Sigma^+ - X^2\Pi$ (0,0) band of the NO product from the H + NO₂ reaction. Individual rotational lines are indicated; rotational branches are designated in Hund's case (b) notation. (b) Simulated spectrum with the NO $v = 0$ rotational populations adjusted to reproduce the experimental spectrum in (a).

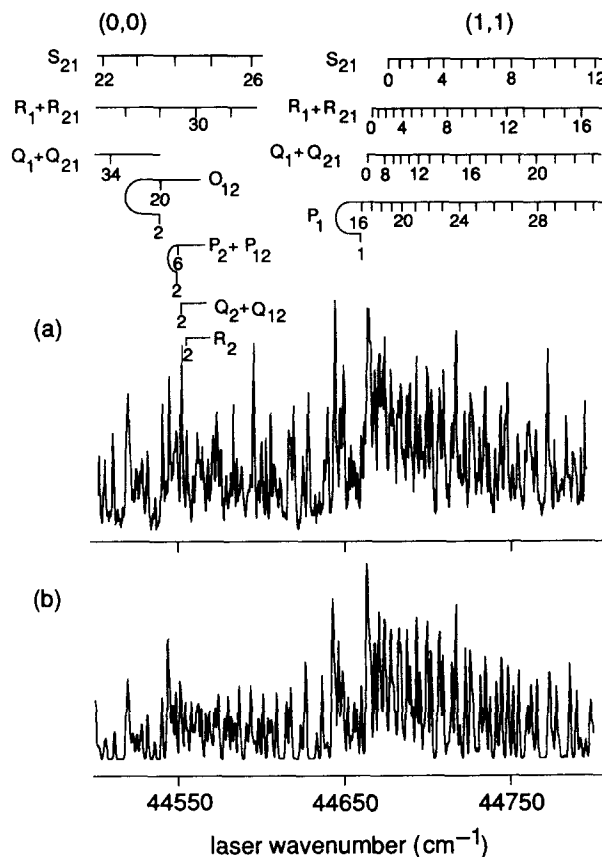


FIG. 2. Experimental laser fluorescence excitation spectrum of the overlapping $A-X$ (0,0) and (1,1) bands of the NO product from the H + NO₂ reaction. All eight distinct rotational branches of the (1,1) band, as well as the S_{21} , $R_1 + R_{21}$, and $Q_1 + Q_{21}$ branches of the (0,0) band, are marked. (b) Simulated spectrum.

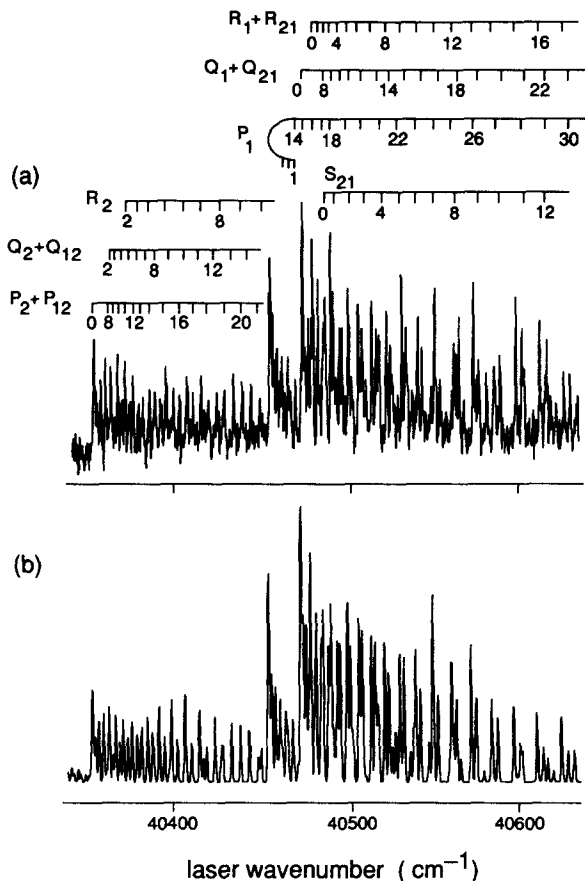


FIG. 3. (a) Experimental laser fluorescence excitation spectrum of the $A-X$ (0,2) band of the NO product from the $H + NO_2$ reaction. (b) Simulated spectrum.

relatively low degree of rotational excitation in NO made it impossible to resolve many of the lines in these excitation spectra. Accordingly, it was not convenient to determine relative rotational populations by measurement of the intensities of individual rotational lines. Therefore, we decided to compare our experimental spectra with simulated ones in order to extract the rotational populations.

The simulated spectra were calculated by convolution of a Gaussian laser line shape of 1.2 cm^{-1} full width at half maximum with the individual laser fluorescence line intensities. The latter were shown by Greene and Zare²⁹ to equal

$$I(v'J'p';vJp) = C\rho(\lambda_{v'J'p';vJp}) \left[\frac{N_{vJp}}{(2J+1)} \right] S_{J'p';Jp} q_{v'v} \\ \times \sum_{J''p''n_d} S_{J'p';J''p''} R_{JJ'J''} \\ \times \sum_{v''} A_{v'v''} P(\lambda_{v'v''}) R(\lambda_{v'v''}). \quad (1)$$

Here N_{vJp} is the population of the p th fine-structure component (spin-orbit + Λ doublet) of a rovibrational (v,J) level, ρ is the laser energy density (energy/cm³) at the wavelength $\lambda_{v'J'p';vJp}$ of the $v'J'p' \leftarrow vJp$ transition, $S_{J'p';Jp}$ is a rotational line strength (Hönl-London) factor,³⁰ and $q_{v'v}$ is the Franck-Condon factor.

The factor $R_{JJ'J''}$ incorporates the dependence of the

LIF signal on the laser and detection polarizations. As discussed in detail by Greene and Zare²⁹ and elsewhere,³¹ this term takes account of the fact that the fluorescence angular distribution varies with rotational branch and only fluorescence into a small solid angle is observed. This factor is given for an isotropic M_J distribution in the detected molecule as^{29,31}

$$R_{JJ'J''} = \left[\frac{1}{9(J'+1)} + \frac{2}{3}(-1)^{J'-J''} \right] \\ \times \left\{ \begin{matrix} J' & J' & 2 \\ 1 & 1 & J \end{matrix} \right\} \left\{ \begin{matrix} J' & J' & 2 \\ 1 & 1 & J'' \end{matrix} \right\} P_2(\cos \chi_{ad}). \quad (2)$$

Here $\{\dots\}$ is a $3j$ symbol.³²

The sum in Eq. (1) over the detector polarizations \hat{n}_d and the final states $v''J''p''$ takes account of the fact that the polarization and wavelength of the fluorescence are not resolved. In Eq. (1), $P(\lambda_{v'v''})$ is the sensitivity of the photomultiplier which was taken from the manufacturer's specifications. $R(\lambda_{v'v''})$ is the reflectivity of the dichroic mirror in the fluorescence telescope at wavelength λ . C is a proportionality constant which includes geometric factors, etc. There have been several recent experimental^{33,34} and theoretical³⁵ studies of the radiative transition probabilities of the NO $A-X$ bands. We have taken values of $q_{v'v}$ and $A_{v'v}$ from the work of Piper and Cowles.³⁴

In the simulations, the rotational populations were parametrized by a cubic spline interpolation constrained to be linear³⁶ in $2J+1$ at low J and smoothly varying over the entire range of J 's considered. Populations in the $\Omega = 1/2$ and $\Omega = 3/2$ spin-orbit manifolds were determined independently. Because the (0,0), (1,1), and (2,2) bands overlap, relative vibrational state populations could be determined directly. Laser intensity decreased rapidly to the blue of the $P_2 + P_{12}$ bandhead in the (2,2) band. We therefore estimated the $v=2$ rotational state distribution from the (0,2) band. The background photolysis signal in the (0,0) band, described earlier, was taken into account by recording spectra with the hydrogen discharge off and on. The NO rotational distribution resulting from the photolysis was determined, and a reactive distribution added to it until the total simulation best reproduced the average of the several experimental scans recorded.

The rotational populations determined to give the best agreement with the experimental Q branch intensities are shown in Fig. 4. The maxima in the rotational distributions shift to slightly lower J 's as the vibrational excitation increases, as would be expected from energy conservation. Extensive variations of the rotational populations were carried out in order to fit the experimental spectra and to probe the sensitivity of the simulations to the populations. Changing the population of an individual J level by less than 20% did not take the simulations out of the range of experimental reproducibility. However, shifting the maxima of the rotational state distributions in Fig. 4 by $\Delta J \pm 2$ yielded simulations which did not match the experimental spectra. It can also be seen from Fig. 4 that the spin-orbit populations are nonstatistical: The lower $\Omega = 1/2$ manifold is significantly preferred over $\Omega = 3/2$. The $\Omega = 1/2$ to $\Omega = 3/2$ popula-

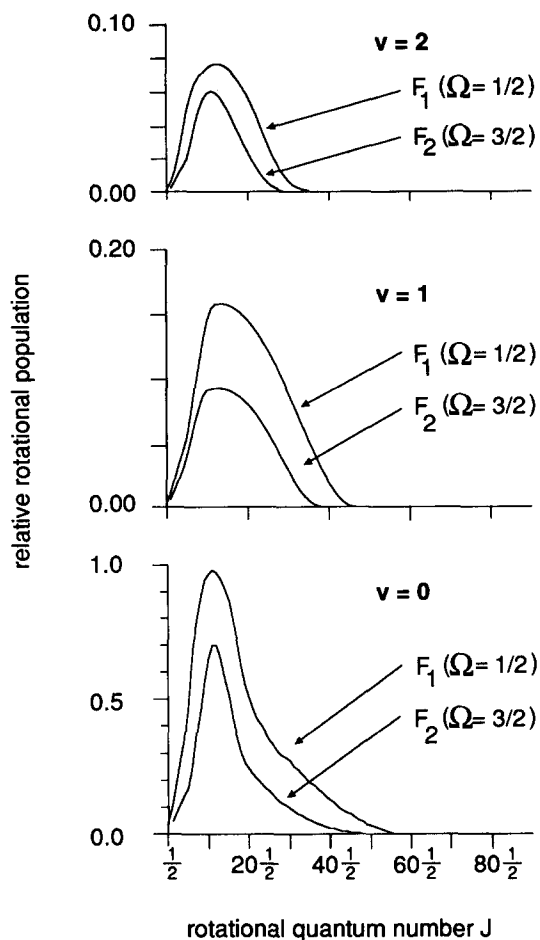


FIG. 4. Experimentally derived vibration-rotation populations for the NO product from the H + NO₂ reaction. These populations are all normalized to the most probable rotational level in the F₁ spin-orbit manifold of the $v = 0$ vibrational level.

tion ratio is $1:0.52 \pm 0.11$. Within the uncertainties in the derived populations, there does not appear to be a variation in the spin-orbit population ratio with v .

Spectral congestion near the bandheads prohibits measurement of line intensities for excitation of individual Λ doublet levels. The $\Pi(A')$ levels are probed in the NO $A^2\Sigma^+ - X^2\Pi$ band system by $\Delta N = \pm 1$ branches, while $\Pi(A'')$ levels are probed by $\Delta N = 0, \pm 2$ branches.^{18,19} In the high- J portion of the (0,0), (1,1), and (0,2) bands, we observed that the intensities of P_1 and R_1 branch lines, as compared to the corresponding Q_1 branch lines, were enhanced over the predicted relative intensities assuming equal Λ doublet populations. Moreover, this enhancement increases with increasing J . Clearly, this implies that the $\Pi(A')$ Λ doublet levels are preferentially populated over the corresponding $\Pi(A'')$ levels in all three vibrational bands. The deduced $\Pi(A')/\Pi(A'')$ ratio reached 2.0 ± 0.5 at $N \approx 50$, the highest rotational levels observed. The nonequal Λ doublet populations were taken into account in generating the simulated spectra in Figs. 1–3.

By summing over the determined individual rotational populations in each vibrational manifold, we find the NO relative vibrational populations, as measured by laser fluorescence detection, equal $1:0.21 \pm 0.04:0.08 \pm 0.03$ for

$v = 0, 1$, and 2 , respectively. The quoted error limits reflect, in part, the uncertainties in comparing the intensities of high- J lines in one band with the bandheads of another vibrational level (see, for example, Fig. 2). The $v = 2$ relative population was subject to greater uncertainty because of the small magnitude of the (2,2) bandheads relative to the high- J lines of the (1,1) band and the small signals in this wavelength range.

As is well known,³⁷ this type of laser fluorescence experiment measures the densities n_f of molecules created in specific quantum states, while the desired quantities, namely cross sections σ_f , are proportional to fluxes. The relationship between these two quantities can be written as^{31,38}

$$n_f = n(\text{H})n(\text{NO}_2)\sigma_f R \langle g/v_f \rangle, \quad (3)$$

where $n(\text{H})$ and $n(\text{NO}_2)$ are the number densities of the reactants in the collision zone, $R = V/\int r^2 d\omega$ is the effective radius of the scattering center. The quantity $\langle g/v_f \rangle$ is the average of the incident relative velocity g divided by the laboratory velocity v_f of the NO product weighted by the c.m. differential cross section:

$$\langle g/v_f \rangle = \int \left(\frac{g}{v_f} \right) \sigma_f^{-1} \left(\frac{d\sigma}{d\omega} \right) d\omega. \quad (4)$$

Even though we are only interested in relative cross sections for production of the NO product states, we must consider Eq. (3) since the quantity $\langle g/v_f \rangle$ varies as a function of the product state.

We can use the measured product angular distribution^{8,9} with Eq. (4) to calculate the variation of $\langle g/v_f \rangle$ as a function of NO internal energy. To simplify this calculation, we have assumed that the NO product recoils in the c.m. frame with a single velocity obtained by subtraction from E_{tot} of the average energy in OH vibration and rotation (50% of E_{tot}) and the NO internal energy. Because of the small amount of energy in NO rotation, the density-flux transformation alters the rotational state distribution within a given vibrational manifold negligibly. The NO $v = 1$ and 2 cross sections relative to that for $v = 0$ must be divided by 1.23 and 1.75, respectively, as compared with the relative vibrational populations reported above. This correction is so large because the NO c.m. velocities are somewhat larger than the velocity of the center of mass of the system and the angular distribution is very broad. We conclude that the product NO vibrational state distribution from the H + NO₂ reaction is given by $1:0.17 \pm 0.04:0.05 \pm 0.02$ for $v = 0, 1$, and 2 , respectively.

IV. DISCUSSION

A. Energy disposal

With the determination of the NO product internal state distribution, we can calculate the average energy which appears as vibrational and rotational excitation of the NO product. We find that approximately 12.1 ± 2.0 kJ/mol, or $(9.5 \pm 2)\%$ of the total energy available to the products, resides as internal excitation of NO. The quoted uncertainty arises from the estimated errors in the internal state distribu-

tion. Over half of this energy, 7.1 ± 1.0 kJ/mol or $(5.6 \pm 1)\%$, appears as rotational excitation. In calculating this energy disposal, we have not attempted to extrapolate the populations of higher vibrational levels ($v > 2$).

The energy disposal we find in NO is considerably less than the 28% energy disposal predicted for NO by subtracting from E_{tot} the average translation energy^{8,9} and average OH product internal excitation derived from previously published results^{7,10-17} on the OH state distribution, as discussed in Sec. I. We are unable to account for this discrepancy. It is disturbing that the expected amount of energy in NO internal excitations is not observed, especially after all the previous work on characterizing the product energy disposal in this reaction. Preliminary results from Smith's laboratory²¹ on the NO state distribution also show an average NO internal excitation considerably less than the expected 28% of the exoergicity. Perhaps these experiments will stimulate further dynamical studies of this important reaction.

As outlined in Sec. I, there seems to be reasonable agreement among the several reports of the vibrational and rotational distributions in the OH product from H + NO₂. The only previously published experimental results on the NO product are from Setser's group.¹² Their most recent study,^{12(c)} in which infrared emission was observed in a fast flow reactor, yielded an NO $v = 1$ to $v = 2$ ratio of 1:0.43, somewhat higher than the $1:0.30 \pm 0.14$ ratio we have observed. We note, however, that there is significant uncertainty in our $v = 2$ relative population.

The H + NO₂ reaction has often been considered to proceed along the lowest $^1A'$ surface, accessing the deep HONO (\tilde{X}^1A') potential well. This suggests that the reaction intermediate might have a lifetime which is sufficiently long to allow randomization of energy disposal in the products. A simple RRK calculation³⁹ of the lifetime of the HONO complex using activated complex frequencies suggested by Anastasi and Smith⁴⁰ predicts a transition state lifetime of $\sim 1 \times 10^{-13}$ s. This is an order of magnitude less than the $\sim 10^{-12}$ s rotational period expected for HONO, indicating that the reaction could be considered to proceed rather directly. The experimentally observed forward peaking of the product angular distribution is consistent with a short lifetime for the complex.

It is also interesting to see whether the reaction exoergicity is distributed statistically in the various product degrees of freedom. We have calculated the product state distributions using phase-space theory, which incorporates angular momentum constraints,^{36,41} on the H + NO₂ system. The rotational distributions derived from that calculation for the NO $v = 0$ to 2 vibrational manifolds are shown in Fig. 5. This theory does not consider the open-shell nature of the reaction products. Because of the relatively small spin-orbit and Λ doublet splittings, statistical distributions are expected for these degrees of freedom. From a comparison of Figs. 4 and 5, we see that our experimental NO rotational state distribution is substantially colder than that predicted by phase-space theory.

Summing over the rotational distributions from the phase-space calculations, we predict that the NO vibrational state populations should be 1:0.66:0.39 for

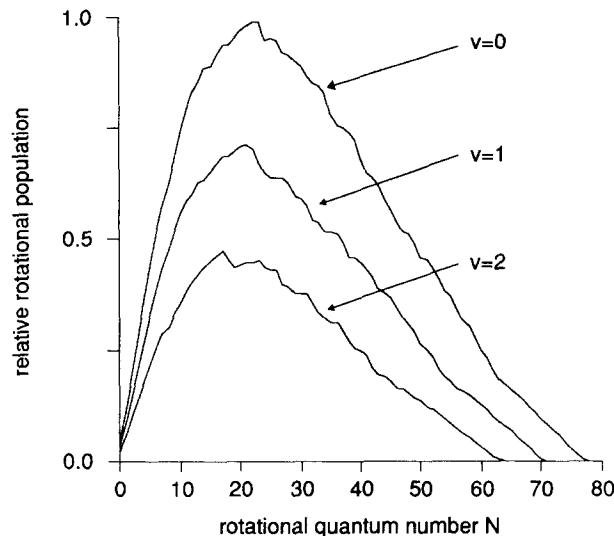


FIG. 5. Vibration-rotation populations calculated by phase-space theory for NO product from the H + NO₂ reaction.

$v = 0:v = 1:v = 2$, respectively. Comparison with our experimentally determined ratios show that the actual vibrational energy release in NO is much less than anticipated for a statistical distribution. Thus, the energy disposal into the NO product for both the vibrational and rotational degrees of freedom is considerably less than that expected if the reaction exoergicity were randomized.

By contrast, the internal state distribution for the OH product is considerably hotter than that predicted by phase-space theory. The calculated phase-space rotational distributions peak at $N = 11$ and 10 for $v = 0$ and 1 , respectively, and the tails extend only to $N = 23$ and 19 . Mariella and Luntz¹⁵ and Silver *et al.*¹⁴ have published experimental OH product rotational distributions which are in good agreement with each other. These experimental distributions peak at $N = 15$ or 16 in $v = 0$, and $N = 12$ for $v = 1$. Predissociation above $N = 16$ in the $v = 1$ level of the upper electronic state prevented observation of the complete nascent rotational distribution in the LIF studies conducted by these two groups. Murphy *et al.*¹⁶ show a flat, broad rotational distribution for the OH $v = 0$ product which extends to $N = 26$.

The OH vibrational state distribution is also observed to be considerably hotter than that predicted by phase-space theory. Using the results from Mariella and Luntz¹⁵ and from Setser's group,¹² the current best estimate for the OH vibrational state distribution is 1:0.70:0.43:0.07 for $v = 0$ to 3, respectively. By contrast, the OH vibrational state population ratios calculated by phase-space theory are 1.0:0.40:0.10:0.002. We thus see that both the vibrational and rotational degrees of freedom of the OH product have significantly more energy than expected from mere statistical considerations. These results for the energy disposal are consistent with our intuition that there should be more energy disposed in the "new" bond (i.e., OH) than in the "old" bond (i.e., NO) in a direct reaction of the type $A + BCD \rightarrow AB + CD$.

B. Λ doublet and spin-orbit populations

Our observation of preferential production of the $\Pi(A')$ levels of the NO product is similar to previous observations^{7,15,16} of preferential formation of the OH $\Pi(A')$ levels. These propensities can be explained^{15,18} by assuming that the reaction proceeds through a planar HONO intermediate of A' symmetry since the overall symmetry of the electronic wave functions of both products should be the same as that of the intermediate. The dissociation of HONO on the \tilde{X}^1A' surface is expected to involve the transformation of the filled molecular orbital⁴² consisting of the bonding combination of the in-plane $2p$ orbitals of the nitrogen and central oxygen atoms into singly occupied π orbitals on each of the products. If planarity is maintained throughout the reactive encounter, then the diatomic products will be rotating in the plane defined by the HONO intermediate, and preferential formation of $\Pi(A')$ levels and Λ doublet levels of both OH and NO is expected, as observed.

It is interesting to speculate on the origin of the preferential production of the F_1 ($\Omega = 1/2$) spin-orbit populations in the NO($X^2\Pi$) product. Unequal spin-orbit populations have also been observed for production of NO in the photodissociation of a number of precursors.^{26,43-49} Similar observations have been reported in the formation of PO from the infrared multiphoton decomposition of organophosphorus compounds,⁵⁰ the production of Σ states in the formation of CN($X^2\Sigma^+$) from ICN (Refs. 51 and 52) and the infrared multiphoton dissociation (IRMPD) of HN₃ to yield NH($X^3\Sigma^-$).^{53,54}

An unequal spin-orbit population implies a preferential orientation of the electron spin relative to an internal molecular axis. If we assume that the H + NO₂ reaction proceeds along the \tilde{X}^1A' surface of HONO, then it is curious that an approximately equal spin-orbit population has been observed¹⁴⁻¹⁶ for the OH product, while a spin-orbit preference is observed here for NO. This difference cannot be caused by energetics since the spin-orbit constants A for OH and NO are approximately the same [120–130 cm⁻¹ (Ref. 55)] and are small compared to the reaction exoergicity. The dissociation of the HONO (\tilde{X}^1A') in and of itself cannot cause a preferential orientation of the electron spins since there is no preferred direction for the electron spins of the nascent NO and OH products on this potential-energy surface.

Unfortunately, little is known about the HONO \tilde{X}^1A' surface except for the region about the equilibrium geometries of the *trans* and *cis* forms from experimental⁶ and computational *ab initio* studies.^{42,56} In fact, there are eight HONO potential-energy surfaces which asymptotically coalesce to yield OH($X^2\Pi$) + NO($X^2\Pi$) products: There are two surfaces each for the classifications $^1,^3A'$ and $^1,^3A''$. Simple wave functions describing these surfaces as the products separate can be constructed by various combinations of OH and NO π orbitals, which can be in or perpendicular to the molecular plane, and the electrons in the two unfilled shells (one on OH and the other on NO) can be singlet- or triplet-spin coupled.

If we define the xz plane to contain the HONO intermediate, then we can describe the wave function of the nascent OH and NO products on the \tilde{X}^1A' surface as

$$|\tilde{X}^1A'\rangle = 2^{-1/2}\{|\pi_i(\text{OH})\bar{\pi}_i(\text{NO})| - |\bar{\pi}_i(\text{OH})\pi_i(\text{NO})|\}, \quad (5)$$

where π_i denotes a π orbital lying in the molecular xz plane. We suppose that the nonstatistical spin-orbit distribution arises from the nonadiabatic coupling of the \tilde{X}^1A' surface with the other surfaces, as occurs in the selective spin-state production of NH($X^3\Sigma^-$) from the IRMPD of HN₃.⁵⁴

As an example of the plausibility of this mechanism for generating spin-orbit selectivity, we consider spin-orbit coupling between \tilde{X}^1A' and the corresponding $^3A'$ wave function, obtained from the triplet-spin coupling of $\pi_i(\text{OH})$ and $\pi_i(\text{NO})$. In the \tilde{X}^1A' state, the electronic wave function is symmetric with respect to reflection of the electronic spin and spatial coordinates through the molecular plane. The spin-orbit operator must also be symmetric with respect to this operation. Since the spatial parts of the \tilde{X}^1A' and $^3A'$ wave functions, and hence their reflection symmetries, are the same, the spatial part of the component of the spin-orbit operator which mixes these two states must also be symmetric. Hence, these wave functions can couple only through the l_y, s_y component. The preceding implies that the \tilde{X}^1A' wave function can only couple to the $^3A'$ component which has the same symmetry with respect to reflection of the electronic spin coordinates through the molecular plane as the initial \tilde{X}^1A' state. Thus, the symmetric \tilde{X}^1A' state can only mix with the symmetric spin component of $^3A'$, which we denote as $|^3A',s\rangle$.

The reflection properties spin functions are summarized in the Appendix of Ref. 54. We can write the wave function for the symmetric component of $^3A'$ as the in-phase combination of $\Sigma = \pm 1$ spin functions:

$$|^3A',s\rangle = 2^{-1/2}\{|\pi_i(\text{OH})\pi_i(\text{NO})| + |\bar{\pi}_i(\text{OH})\bar{\pi}_i(\text{NO})|\}. \quad (6)$$

This spin-orbit mixing will lead to an admixture of $|^3A',s\rangle$ into the wave function describing the dissociating products. Depending on the relative phases of this admixture and the initial \tilde{X}^1A' wave function there will no longer be an equal probability for the electron spin to be up or down on the NO or OH. In other words, the expectation value for the projection of the OH and NO electron spins onto the quantization axis z in the HONO intermediate will not be zero, implying a preferential orientation of the spins. It is important to note that this spin alignment will be manifest along a molecule-fixed, and not space-fixed, axis since it is the molecule-fixed l_y, s_y component of the spin-orbit operator which causes the mixing.

The preceding paragraphs have described how an orientation of the electron spins might be generated in the nascent OH and NO products. This will only lead to an unequal spin-orbit population in a free diatomic product if it does not rotate too rapidly as the complex is dissociating so that the preferred orientation along the quantization axis in the HONO complex can be transferred to the molecular axis in the free diatom. In this regard, OH and NO differ significantly in that the former is close to Hund's case (b) coupling, while the latter is well described by case (a). In these

two limiting situations, the electron spin is weakly and strongly coupled to the diatomic molecular axis, respectively. Thus, it is reasonable that no spin-orbit preference is observed for OH since the molecular rotation would be expected to wash out any preferred orientation in the molecular frame.

Of course, the model presented above is simplistic in that no details about the HONO surfaces are considered. Clearly, there can be coupling of the \tilde{X}^1A' surface to all the other surfaces asymptotically coalescing to the OH + NO exit channel. Moreover, it is not even possible to predict in the present qualitative treatment of $\tilde{X}^1A'-^3A'$ mixing which spin-orbit component of the NO product will be preferred. Perhaps it will be feasible in the future to carry out quantitative calculations for the modeling of the preferential formation spin-orbit states. This will require knowledge about the adiabatic energies and the nonadiabatic couplings of these surfaces.

ACKNOWLEDGMENTS

The authors are indebted to J. P. Doering for help in the construction of the extended Evenson-Broida microwave cavity used for the generation of hydrogen atoms and to I. W. M. Smith and D. W. Setser for conversations and correspondence concerning their work on the H + NO₂ reaction. We also appreciate discussions with D. R. Yarkony on spin-orbit coupling. This paper has benefitted from incisive criticisms by the referee. This research was supported by the National Science Foundation under Grant No. CHE-8700970 and by the U.S. Army Research Office under Contract No. DAAL03-88-K-0031.

- ¹ M. W. Chase, Jr., C. A. Davies, J. R. Downey, Jr., D. J. Frurip, R. A. McDonald, and A. N. Syverud, *J. Phys. Chem. Ref. Data* **14**, Suppl. 1 (1985).
- ² M. A. A. Clyne and P. B. Monkhouse, *J. Chem. Soc. Faraday Trans. 2* **73**, 298 (1977); P. P. Bemand and M. A. A. Clyne, *ibid.* **73**, 394 (1977).
- ³ H. G. Wagner, U. Welzbacher, and R. Zellner, *Ber. Bunsenges. Phys. Chem.* **80**, 1023 (1976).
- ⁴ J. V. Michael, D. F. Nava, W. A. Payne, J. H. Lee, and L. J. Steif, *J. Phys. Chem.* **83**, 2818 (1979).
- ⁵ M. A. A. Clyne, in *Reactive Intermediates in the Gas Phase*, edited by D. W. Setser (Academic, New York, 1979), p. 2.
- ⁶ L. H. Jones, R. M. Badger, and G. E. Moore, *J. Chem. Phys.* **19**, 1599 (1951); G. E. McGraw, D. L. Bernitt, and I. C. Hisatsune, *ibid.* **45**, 1392 (1966).
- ⁷ R. P. Mariella, Jr., B. Lantzsch, V. T. Maxson, and A. C. Luntz, *J. Chem. Phys.* **69**, 5411 (1978).
- ⁸ H. Haberland, P. Rohwer, and K. Schmidt, *Chem. Phys.* **5**, 298 (1974); H. Haberland, W. von Lucadou, and P. Rohwer, *Ber. Bunsenges. Phys. Chem.* **84**, 507 (1980).
- ⁹ E. J. Murphy, J. H. Brophy, and J. L. Kinsey, *J. Chem. Phys.* **74**, 331 (1981).
- ¹⁰ J. C. Polanyi and J. J. Sloan, *Int. J. Chem. Kinet. Symp.* **1**, 51 (1975).
- ¹¹ G. K. Smith and E. R. Fisher, *J. Phys. Chem.* **82**, 2139 (1978).
- ¹² (a) B. S. Agrawalla, A. S. Manocha, and D. W. Setser, *J. Phys. Chem.* **85**, 2873 (1981); (b) M. A. Wickramaaratchi, D. W. Setser, B. Hilderbrandt, B. Korbitzer, and H. Heydtmann, *Chem. Phys.* **84**, 105 (1984); (c) S. J. Wategaonkar and D. W. Setser, *J. Chem. Phys.* **90**, 251 (1989).
- ¹³ D. Klenerman and I. W. M. Smith, *J. Chem. Soc. Faraday Trans. 2* **83**, 229 (1987).
- ¹⁴ J. A. Silver, W. L. Dimpfl, J. H. Brophy, and J. L. Kinsey, *J. Chem. Phys.* **65**, 1811 (1976).
- ¹⁵ R. P. Mariella, Jr. and A. C. Luntz, *J. Chem. Phys.* **67**, 5388 (1977).

- ¹⁶ E. J. Murphy, J. H. Brophy, G. S. Arnold, W. L. Dimpfl, and J. L. Kinsey, *J. Chem. Phys.* **74**, 324 (1981).
- ¹⁷ J. E. Spencer and G. P. Glass, *Chem. Phys.* **15**, 35 (1976).
- ¹⁸ M. H. Alexander and P. J. Dagdigian, *J. Chem. Phys.* **80**, 4325 (1984).
- ¹⁹ M. H. Alexander, P. Andresen, R. Bacis, R. Bersohn, F. J. Comes, P. J. Dagdigian, R. N. Dixon, R. W. Field, G. W. Flynn, K.-H. Gericke, E. R. Grant, B. J. Howard, J. R. Huber, D. S. King, J. L. Kinsey, K. Kleiner-manns, K. Kuchitsu, A. C. Luntz, A. J. McCaffery, B. Pouilly, H. Reisler, S. Rosenwaks, E. W. Rothe, M. Shapiro, J. P. Simons, R. Vasudev, J. R. Wiesenfeld, C. Wittig, and R. N. Zare, *J. Chem. Phys.* **89**, 1749 (1988).
- ²⁰ A. M. L. Irvine, I. W. M. Smith, R. P. Tuckett, and X.-F. Yang, *J. Chem. Phys.* (submitted).
- ²¹ A. M. L. Irvine, I. W. M. Smith, and R. P. Tuckett, *J. Chem. Phys.* (submitted).
- ²² P. J. Dagdigian, *J. Chem. Phys.* **90**, 2617 (1989); **90**, 6110 (1989); D. G. Sauder, D. Patel-Misra, and P. J. Dagdigian, *ibid.* **91**, 5316 (1989).
- ²³ E. J. Murphy and J. H. Brophy, *Rev. Sci. Instrum.* **50**, 635 (1979).
- ²⁴ R. E. Smalley, L. Wharton, and D. H. Levy, *J. Chem. Phys.* **63**, 4977 (1975).
- ²⁵ C. A. Wight, D. J. Donaldson, and S. R. Leone, *J. Chem. Phys.* **83**, 660 (1985).
- ²⁶ D. C. Jacobs, R. J. Madix, and R. N. Zare, *J. Chem. Phys.* **85**, 5469 (1986).
- ²⁷ M. Noble, C. X. W. Qian, H. Reisler, and C. Wittig, *J. Chem. Phys.* **85**, 5763 (1986).
- ²⁸ R. Engleman, P. E. Rouse, H. M. Peck, and V. D. Baiamonte, Los Alamos Scientific Laboratory, Report No. LA-4364, 1970.
- ²⁹ C. H. Greene and R. N. Zare, *J. Chem. Phys.* **78**, 674 (1983).
- ³⁰ R. N. Zare, in *Molecular Spectroscopy: Modern Research*, edited by K. N. Rao and C. W. Mathews (Academic, New York, 1972), p. 207.
- ³¹ P. J. Dagdigian, in *Atomic and Molecular Beam Methods*, edited by G. Scoles, D. Bassi, U. Buck, and D. Lainé (Oxford U. P., New York, 1988), Vol. 1, Chap. 24.
- ³² D. M. Brink and G. R. Satchler, *Angular Momentum*, 2nd ed. (Academic, New York, 1968).
- ³³ T. J. McGee, G. E. Miller, J. Burris, Jr., and T. J. McIlrath, *J. Quant. Spectrosc. Radiat. Transfer* **29**, 333 (1983); T. J. McGee, J. Burris, Jr., and J. Barnes, *ibid.* **34**, 81 (1985).
- ³⁴ L. G. Piper and L. M. Cowles, *J. Chem. Phys.* **85**, 2419 (1986).
- ³⁵ S. R. Langhoff, C. W. Bauschlicher, Jr., and H. Partridge, *J. Chem. Phys.* **89**, 4909 (1988).
- ³⁶ P. J. Dagdigian, H. W. Cruse, A. Schultz, and R. N. Zare, *J. Chem. Phys.* **61**, 4450 (1974).
- ³⁷ H. W. Cruse, P. J. Dagdigian, and R. N. Zare, *Faraday Discuss. Chem. Soc.* **55**, 277 (1973).
- ³⁸ H. Joswig, P. Andresen, and R. Schinke, *J. Chem. Phys.* **85**, 1904 (1986).
- ³⁹ P. J. Robinson and K. A. Holbrook, *Unimolecular Reactions* (Wiley-Interscience, London, 1972).
- ⁴⁰ C. Anastasi and I. W. M. Smith, *J. Chem. Soc. Faraday Soc. 2* **74**, 1056 (1978).
- ⁴¹ P. Pechukas, J. C. Light, and C. Rankin, *J. Chem. Phys.* **44**, 794 (1966).
- ⁴² See, for example, P. Benioff, G. Das, and A. C. Wahl, *J. Chem. Phys.* **64**, 710 (1976).
- ⁴³ F. Lahmani, C. Lardeux, and D. Solgadi, *Chem. Phys. Lett.* **129**, 24 (1986).
- ⁴⁴ U. Brühlmann and J. R. Huber, *Chem. Phys. Lett.* **143**, 199 (1988).
- ⁴⁵ L. Bigio and E. R. Grant, *J. Phys. Chem.* **89**, 5855 (1985); *J. Chem. Phys.* **87**, 360 (1987); **87**, 5589 (1987).
- ⁴⁶ D. S. King and J. C. Stephenson, *J. Chem. Phys.* **82**, 2236 (1985).
- ⁴⁷ D. Schwartz-Lavi and S. Rosenwaks, *J. Chem. Phys.* **88**, 6922 (1988).
- ⁴⁸ R. Lavi and S. Rosenwaks, *J. Chem. Phys.* **89**, 1416 (1988).
- ⁴⁹ C. G. Atkins and G. Hancock, *Laser Chem.* **9**, 195 (1988).
- ⁵⁰ J.-S. Chou, D. S. Sumida, and C. Wittig, *J. Chem. Phys.* **82**, 1376 (1985).
- ⁵¹ I. Nadler, D. Mahgerefteh, H. Reisler, and C. Wittig, *J. Chem. Phys.* **82**, 3885 (1985).
- ⁵² H. Joswig, M. A. O'Halloran, R. N. Zare, and M. S. Child, *J. Chem. Phys.* **82**, 83 (1986).
- ⁵³ J. C. Stephenson, M. P. Casassa, and D. S. King, *J. Chem. Phys.* **89**, 1378 (1988).
- ⁵⁴ M. H. Alexander, H.-J. Werner, and P. J. Dagdigian, *J. Chem. Phys.* **89**, 1388 (1988).
- ⁵⁵ K. P. Huber and G. Herzberg, *Molecular Structure and Molecular Structure IV. Constants of Diatomic Molecules* (Van Nostrand Reinhold, New York, 1979).
- ⁵⁶ A. G. Turner, *J. Phys. Chem.* **89**, 4480 (1985), and references therein.